IAC-15- C2.9.3

MATERIALS CHARACTERIZATION OF ADDITIVELY MANUFACTURED COMPONENTS FOR ROCKET PROPULSION

Robert Carter
National Aeronautics and Space Administration, Glenn Research Center, U.S.A., robert.carter@nasa.gov

Susan Draper, Ivan Locci, Bradley Lerch, David Ellis, Paul Senick, Michael Meyer, James Free
National Aeronautics and Space Administration, Glenn Research Center, U.S.A.

Ken Cooper, Zachary Jones
National Aeronautics and Space Administration, Marshall Space Flight Center, U.S.A.

To advance Additive Manufacturing (AM) technologies for production of rocket propulsion components the NASA Glenn Research Center (GRC) is applying state of the art characterization techniques to interrogate microstructure and mechanical properties of AM materials and components at various steps in their processing. The materials being investigated for upper stage rocket engines include titanium, copper, and nickel alloys. Additive manufacturing processes include laser powder bed, electron beam powder bed, and electron beam wire fed processes. Various post build thermal treatments, including Hot Isostatic Pressure (HIP), have been studied to understand their influence on microstructure, mechanical properties, and build density. Micro-computed tomography, electron microscopy, and mechanical testing in relevant temperature environments has been performed to develop relationships between build quality, microstructure, and mechanical performance at temperature. A summary of GRC's Additive Manufacturing roles and experimental findings will be presented.

I. INTRODUCTION

Additive Manufacturing (AM) is revolutionizing the design and manufacture of rocket engines. Incremental deposition of material, layer-by-layer, using AM allows for new designs that are unattainable using conventional subtractive machining techniques. Additionally, AM enables rapid and inexpensive production of high fidelity hardware prototypes. This permits more efficient testing and iteration of design solutions to achieve desired performance characteristics.

Recently AM processes have achieved a level of maturity where they are capable of producing metallic flight quality hardware components. The leading technology in this area is Powder Bed Fusion (PBF) where metallic powder is selectively fused layer by layer using either an electron beam in Electron Beam Melting (EBM), or laser beam in Laser Beam Melting (LBM).

Multiple factors can affect the properties of metallic components produced using PBF. These include powder feedstock chemistry and morphology, processing parameters used during the build, and post processing thermal processes. Researchers at the NASA Glenn Research Center (GRC) are interrogating the microstructure and mechanical properties of components produced using PBF. The results of studies conducted on titanium alloy Ti-6Al-4V for an RL10 rocket engine component and on copper alloy GRCop-84 for a low cost upper stage rocket engine are covered in detail. Hot fire testing performed at GRC is also discussed.

II. GRC AND ADDITIVE MANUFACTURING

GRC has an extensive heritage in the research, testing, and development of rocket engine technology and in the development of materials for extreme environments. GRC's expertise in high temperature alloy

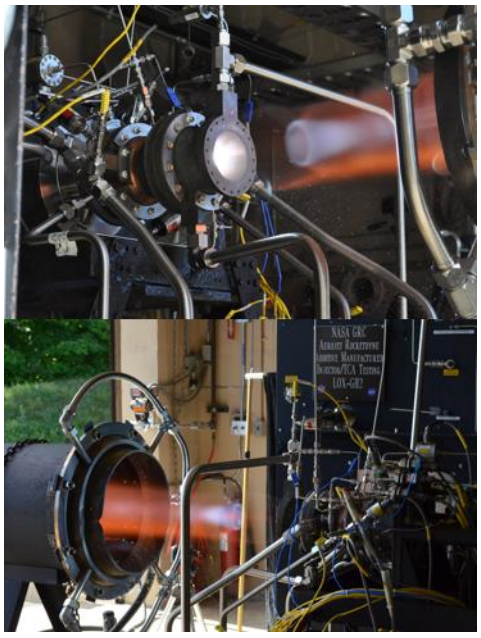

Fig. 1: Hot Fire Testing of Additively Manufactured Hardware at GRC.

development and performance is of intrinsic value to the advancement of AM for rocket components. GRCs role in these AM efforts addresses the relationships between materials processing and materials microstructure and performance in order to support manufacturing efforts developing robust components for this challenging application. GRC's investigations are also obtaining statistical data to develop databases important for AM specifications and standards.

Other NASA Centers, other government agencies, and U.S. industry have partnered with GRC in efforts to manufacture and characterize challenging components for space propulsion. These efforts are providing unique insight into AM as applied to aerospace materials and components. This paper will describe GRC's roles and results conducted under recent partnerships including:

- RL10 AM System Study with Aerojet Rocketdyne
- Hot Fire Test of Aerojet Rocketdyne Copper Thrust Chamber Assembly.
- Materials Characterization of Ti-6Al-4V in cooperation with the U.S. Air Force and Aerojet Rocketdyne.
- Materials Characterization for a Low Cost Upper Stage Engine with NASA MSFC and NASA LaRC.

III HOT FIRE TESTING

With funding provided by the NASA Space Technology Mission Directorate, Game Changing Development Program, GRC and Aerojet Rocketdyne partnered to perform hot fire testing of a sub-scale rocket engine thrust chamber with full-scale RL10 features. See Figure 1.

This testing utilized an AM Ni-alloy injector and an AM copper alloy thrust chamber. The test configuration was designed to enable change out of components to enable testing various configurations. Four different configurations were tested in 19 tests.

Among the significant outcomes of this work was verification of the functional requirements of an AM component, which has paved the way for full-scale implementation into the RL10 engine. Additionally, this work identified the potential for improved performance and cost savings associated with AM as applied to specific engine components. Finally, this work was among the first hot fire testing of copper alloy hardware produced using AM.

IV. ELECTRON BEAM MELTED TI-6AL-4V

In cooperation with the United States Air Force and Aerojet Rocketdyne, NASA GRC has generated a material database for EBM Ti-6Al-4V. While Ti-6Al-4V has been manufactured by electron beam melting for a number of years, a database of microstructure and corresponding mechanical properties from cryogenic to elevated temperatures was needed for component design. A complete database, including low cycle fatigue, fatigue crack growth, fracture toughness and thermal properties has been generated [1, 2].

Material and Test Procedure

The EBM Ti-6Al-4V material was fabricated using an Arcam A2X EBM machine. Samples were fabricated under eight separate builds with the material divided into two lots for material testing purposes. Specimens were fabricated vertically for the majority of the specimens, but one build for a smaller group of samples was performed horizontally.

Chemical analysis was performed on the raw powder, and on EBM samples both pre and post HIP treatment. For these analysis O and N were determined by LECO fusion, C by LECO combustion, and all others by Inductively Coupled Plasma (ICP) Atomic Emission.

Crystallographic texture was acquired from polished samples using a Bruker D8 Discover x-ray diffractometer equipped with a sealed Cu tube, graphite monochrometer set to Ka radiation, 0.5mm diameter collimator, and Vantec 500 area detector. Data was acquired for the α-Ti (100), (002), (101), (102), (110), (103), (112), and (201) poles at 5° resolution.

All mechanical test samples were Hot Isostatically Pressed (HIP) to close internal porosity. Tensile tests were performed in strain control at a rate of

	Ti	Al	V	C	O	N	Fe	Cr	Si
Powder	Bal.	6.57	3.98	0.008	0.23	0.022	0.13	0.008	0.01
As Fabricated	Bal.	6.01	3.87	0.009	0.23	0.023	0.12	0.007	0.009
Post HIP, Lot 1,	Bal.	6.26	3.93	0.009	0.23	0.021	0.11	0.007	0.011
Post HIP, Lot 2,	Bal.	5.92	3.89		0.25	0.022	0.10	0.006	0.009
Post HIP,	Bal.	6.2	3.97		0.26	0.023	0.14	0.007	0.013
ASTM F2924	Bal.	5.5-6.75	3.5-4.5	Max. 0.08	Max. 0.2	Max. 0.05	Max. 0.30	Max. 0.1	Max. 0.1

Table 1: Ti-6Al-4V Chemistry (wt%)

.0001/sec. High Cycle Fatigue (HCF) tests were conducted in load control at a frequency of 20-30 Hz. Tests were performed using a sinusoidal waveform at three load ratios, R_σ , of -1, 0.1, and 0.5 and test temperatures of -196, 20, and 149ºC. Ten million cycles was the runout value for the long-term tests. The crack origin(s) on every sample was identified using optical microscopy and Scanning Electron Microscopy (SEM).

Results and Discussion

The chemistry of the starting powder and fabricated samples was analyzed and is shown in Table I. The same batch of starting powder was used for all builds. Compositions were compared to ASTM Standard F2924, "Standard Specification for Additive Manufacturing Titanium-6 Aluminum-4 Vanadium with Powder Bed Fusion." and results are shown in Table I. The oxygen content of the starting powder was above the ASTM standard limit and remained there after fabrication and HIP. All other elements were within the specification range.

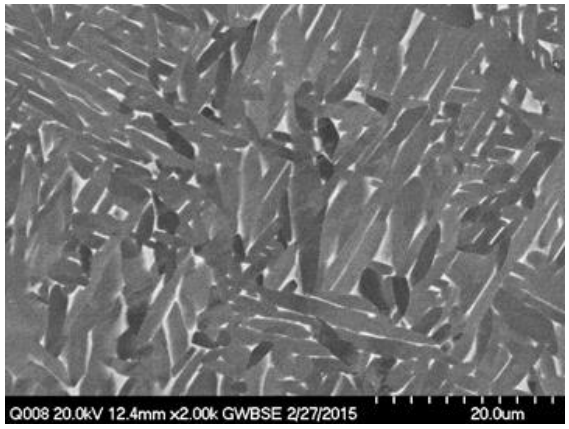

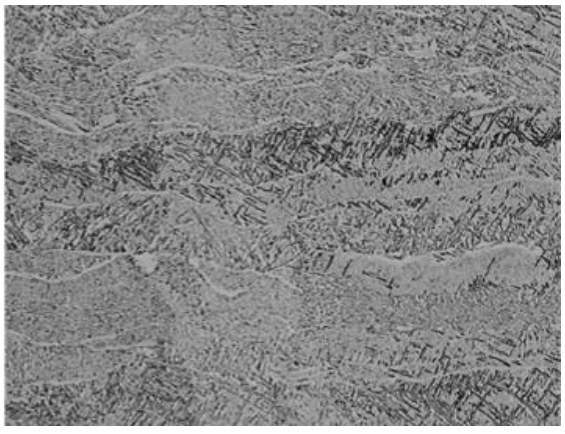

Fig 2 and 3: Figure 2 (top) shows SEM image transverse to the growth direction. Figure 3 (bottom) shows optical image in longitudinal direction.

In the as-fabricated state, the samples contained a population of porosity that was detected by computed tomography (CT) and metallography. Pore size was measured on a metallographic sample and averaged 33 ± 4 μm, with pore size ranging from 7 to 106 μm. Following HIP, CT and metallography confirmed full porosity closure.

The post HIP microstructure consisted of columnar prior β grains and a transformed α + β microstructure, Figure 2. The columnar microstructure is best observed in optical micrographs of longitudinal samples etched with Kroll's reagent used as an etchant to reveal structural features, Figure 3.

X-ray diffraction was used to determine the presence of preferential crystal structure orientation, referred to as texture. Lot 1 samples had a fiber texture with hexagonal base planes of the α phase orientated perpendicular to the growth direction, Figure 4. Lot 2 samples had no preferred orientation and the horizontal samples had coexisting (100), (002), and (101) α – fiber texture with all 3 fiber axes parallel to the build direction.

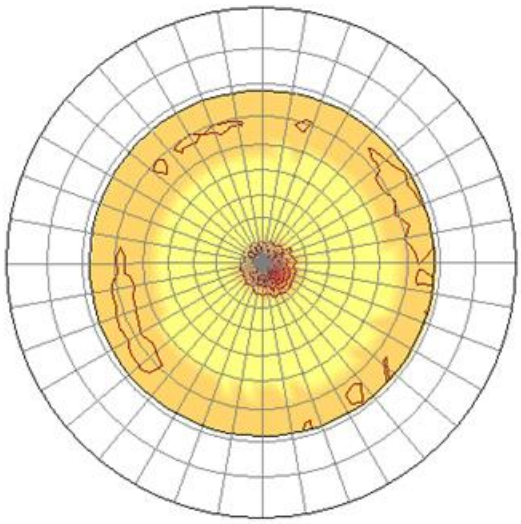

Fig. 4: (002) pole figure from lot 1 showing fiber texture in the build direction.

Representative tensile curves from lot 1 and 2 samples at each temperature as well as a horizontal sample are shown in Figure 5. The strength of the material decreases and the ductility increases with increasing temperature. The elastic modulus, 0.2 % offset yield strength (YS) and ultimate tensile strength (UTS) were higher for lot 1 than lot 2 samples with the difference being consistent over the entire temperature range. The horizontal samples had similar strength to lot 2 samples at room temperature (RT) but had lower ductility, averaging 13.4% failure strain. Metallic Materials Properties Development and Standardization

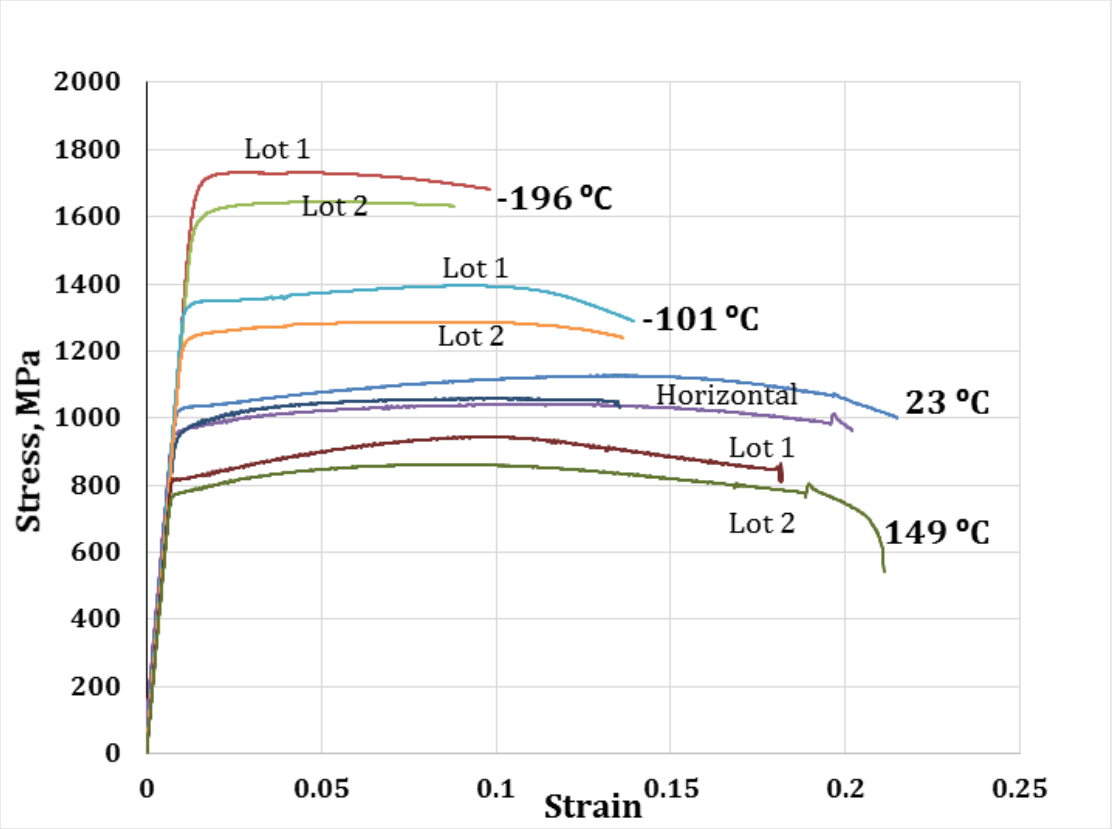

Fig. 5: Representative tensile curves.

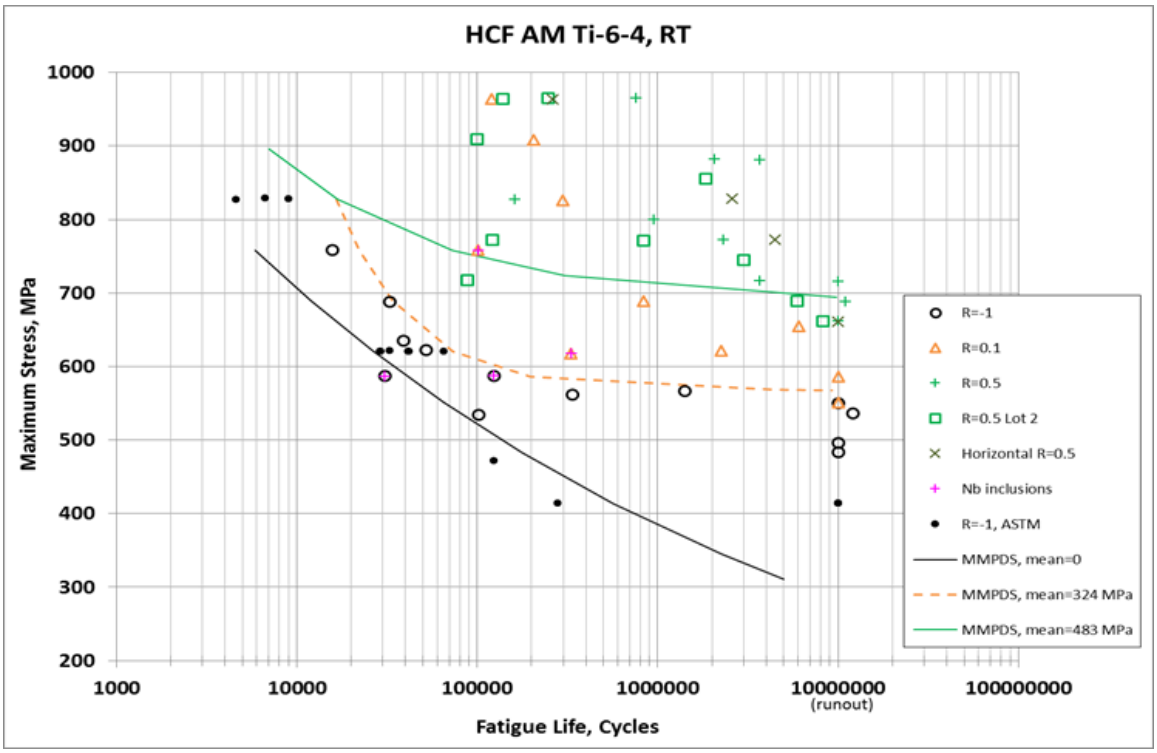

Fig. 6: Room Temperature High Cycle Fatigue Data

(MMPDS) cites a minimum property value (see S-basis) for annealed extrusions as having an UTS of 896 MPa and failure strains of 10 percent. All of the AM samples exceeded these values with the exception of the failure strain for one sample that failed at a low-density inclusion containing Si, Al, O, and Ca.

The difference in strength between lots 1 and 2 can only be explained by the difference in texture. (002) fiber texture has been shown to increase the strength of Ti-6Al-4V[3]. The samples were fabricated within days of each other using the same build parameters. It's not clear why lot 1 had a fiber texture and lot 2 had a random texture.

The difference in strength for the horizontal samples could be explained by the larger α phase colony size and lath thickness. Slip length is effectively controlled by the colony size[4,5]. Larger colonies allow for longer slip and slightly lower strengths. Additionally, the α phase present at the β grain boundaries was perpendicular to the tensile axis. The α phase exhibited a brittle appearance on the fracture surfaces of the horizontal samples and is likely the cause of the lower ductility.

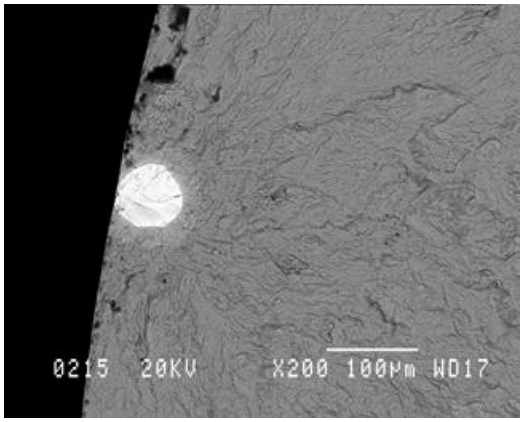

Fig. 7: Nb inclusion at HCF initiation site

A summary of 20˚C HCF results is given in Figure 6. Noted on this figure are samples that failed from Nb inclusions, Figure 7. These inclusions were detected with NDE and noted as high-density inclusions scattered throughout all the samples. The inclusions appear to be round powder particles and contain only Nb. The Arcam system utilized was a dedicated Ti-6Al-4V system and no other alloy has ever been melted in this system. It is believed the Nb came from the starting powder.

Data for the three load ratios (R_σ = -1, 0.1, and 0.5) are plotted with specific colors; black for R=-1, orange for 0.1, and green for .5. At R=-1, the fatigue limit of the AM material is 550 MPa, significantly higher than the fatigue limit of approximately 350 MPa for MMPDS data. This trend is understandable since the UTS for the lot 1 material is 1130 MPa and for the MMPDS is only 945 MPa, a 185 MPa difference. At R=0.1 the AM data lie completely above the fit line from the MMPDS data. The fatigue limits from both are similar, but the AM has much longer lives at all other stress values for the same maximum stresses. Even the two samples that failed prematurely from surface connected, Nb-inclusions had longer lives than those taken from MMPDS. Finally, at a load ratio of 0.5 the AM samples showed equivalent or better lives than the MMPDS fit, especially at higher stresses. The fatigue limits for the AM samples are similar to those from MMPDS but slightly (6 percent) lower for the limits from lot 2 and the horizontal build. However, the data are sparse in this regime. At the higher stress levels (>700 MPa) the data from R=0.1 and 0.5 are very similar indicating that the maximum stress rather than the stress range or mean stress drives the fatigue life. HCF results from cryogenic and elevated temperature are given in the projects final report [1].

V. LASER BEAM MELTED GRCop-84

GRCop-84 (Cu-8 at.% Cr-4 at.% Nb) was developed at NASA GRC for use in reusable launch vehicles and hypersonic craft. Its primary attributes are retention of high temperature strength to 700 °C, excellent creep resistance and excellent low cycle fatigue resistance while retaining a high thermal conductivity[6]. The good mechanical properties and thermal stability exhibited by the alloy comes from a fine dispersion of Cr_2Nb particles. This high melting point intermetallic compound uses two elements with minimal solid solubility in solid copper to minimize coarsening. A slight excess of Cr is specified to minimize the activity of Nb in the alloy and prevent hydrogen embrittlement. Prior work has shown that the alloy is highly adaptable and can be processed by virtually any means desired[7]. The current effort is designed to extend processing to include Laser Beam Melting (LBM) and to characterize the resulting microstructure and mechanical properties.

While these activities are still largely ongoing, significant observations of the GRCop-84 microstructure and the effects of LBM processing parameters, and subsequent HIPing are presented in this paper.

Material and Test Procedure

In total eighteen GRCop-84 melts have been produced. Powder chemistry from the initial four melts is presented here. Results from analytical chemical analysis are shown in Table 2. Data from the powder vendor's certification documentation and NASA GRC's analytical chemistry lab are included. Examination of the oxygen content reveals an apparent increase in oxygen content between the vendor's certification measurements and NASA's in-house measurements. Overall the powder chemistry, in particular the Cr/Nb ratio, was within the range specified. The impurity elements identified are in the part-per-million range, and are not expected to result

		Melt 522-401				Melt 522-403					Melt 522-404				Melt 522-405			
Element	Spec	From ATI	Bottle 1	Bottle 2	Bottle 9	From ATI	Bottle 6	Bottle 7	Bottle 10	Bottle 12	From ATI	Bottle 3	Bottle 8	Bottle 11	From ATI	Bottle 4	Bottle 5	Element
Cu	Balance	Balance	Balance	Balance	Balance	Balance	Balance	Balance	Balance	Balance	Balance	Balance	Balance	Balance	Balance	Balance	Balance	Cu
Cr	6.2-6.8	6.2	6.30	6.30	6.26	6.59	6.59	6.64	6.59	6.66	6.55	6.61	6.58	6.58	6.45	6.63	6.65	Cr
Nb	5.4-6.0	5.72	5.84	5.83	5.83	5.75	5.81	5.85	5.82	5.87	5.64	5.80	5.79	5.79	5.61	5.83	5.84	Nb
Cr/Nb	1.08-1.21	1.08	1.08	1.08	1.07	1.15	1.13	1.14	1.13	1.13	1.16	1.14	1.14	1.14	1.15	1.14	1.14	Cr/Nb
Al		<.004	0.006	0.013	0.004	0.006	0.016	0.009	0.007	0.005	<.004	0.011	0.008	0.008	<.004	0.01	0.004	Al
Ca			0.0001	0.0005	0.0045	<.004	0.0027	0.0008	0.0018	0.0024	<.004		0.001	0.001	<.004			Ca
Fe	.02 max	<.004	0.004	< 0.001	0.003	0.004	0.006	0.004	0.011	0.004	<.004	0.001	0.001	0.001	<.004	0.003	0.002	Fe
Ni		<.001					0.016	0.016	0.027	0.016								Ni
Si		0.01	0.005		0.004	0.007	0.003	0.001	0.013	0.002	0.006		0.002	0.002	0.004	0.003		Si
Ti				0.01			0.004						0.005	0.005		0.01		Ti
Y		<.005	0.001			<.005	0.002		0.0003		<.005				<.005		0.0001	Y
Zr			0.001	0.001	0.001	<.005	0.002	0.002	0.002	0.002	<.004	0.001	0.001	0.001	<.004	0.003	0.002	Zr
C		0.003	0.005	0.006	0.005	0.002	0.004	0.005	0.005	0.007	0.002	0.003	0.004	0.004	0.002	0.004	0.004	C
N			< 0.001	< 0.001	< 0.001	0.002	0.0016	0.0014	0.0015	0.0014	<.001	< 0.001	< 0.001	< 0.001	<.001	0.0013	0.0011	N
O	0.07 max	0.053	0.079	0.070	0.067	0.065	0.066	0.076	0.069	0.085	0.052	0.061	0.066	0.066	0.058	0.091	0.072	O

Table 2: GRCop-84 Starting Powder Chemistry (wt%)

	Powder Specification	Average Chemisry of powder	Sample TO2-6-1800 Pre-HIP	Sample TO2-6-1800 Post-HIP	Sample TO4-625 Pre-HIP	Sample TO4-625 Post-HIP
Cu	Balance	Balance	Balance	Balance	Balance	Balance
Cr	6.2-6.8	6.533	6.720	6.800	6.540	6.740
Nb	5.4-6.0	5.825	5.950	6.070	6.100	6.100
CR/Nb	1.08-1.21	1.121	1.129	1.120	1.072	1.105
Al		0.008				
Ti		0.007				
Y		0.001				
Ca		0.002	0.001	0.002	0.001	0.002
Fe	.02 max	0.004	0.002	0.003	0.002	0.003
Mg		0.019	0.001	0.001	0.000	0.001
Na		0.004	0.000	0.001	0.000	0.001
Ni		0.007	0.003	0.007	0.003	0.004
Si		0.001	0.006	0.010	0.010	0.012
Zr		0.002	0.002	0.002	0.001	0.001
C		0.005	0.0014, 0.0014	0.0030, 0.0034	0.0015, 0.0019	0.0022, 0.0025
O	0.07 max	0.072	0.060, 0.059	0.066, 0.061	0.066, 0.064	0.066, 0.065

Table 3: Analytical chemistry results pre and post HIP (wt%)

in deleterious metallurgical phases or a decrease in mechanical properties.

Results and Discussion:

Analytical chemistry was performed to examine changes in oxygen content due to processing. Analysis was conducted on the starting powder and on LBM produced samples before and after HIPing. The results of this analysis are shown in Table 3 and indicate that there is no significant pickup of oxygen during processing. The table includes data for the average powder composition, and for two representative samples pre and post-HIPing.

Fig. 8: Example of GRCop-84 samples used for analysis.

To establish build parameters Engineers at the NASA Marshall Space Flight Center (MSFC) produced several sets of GRCop-84 specimens for analysis Figure 8. All specimens were analyzed using optical microscopy and Computed Tomography (CT) in order to guide MSFC in the selection of build parameters for the chamber. Photomicrographs of the extreme processing parameters are shown in Figures 9 and 10. From these images it can be seen that build quality, and in particular porosity, are strongly dependent on processing parameters.

Hot Isostatic Pressing (HIPing) will be performed on the combustion chamber liner in order to close pores, anneal the microstructure, and relieve residual stresses from the build process. To evaluate the results of HIP processing, samples produced using multiple parameter sets were HIPed. Optical microscopy of specimens after HIPing confirmed that very little porosity remained in the microstructure. Additionally, CT was performed both pre- and post-HIP. These CT results indicated that very little, if any, porosity larger than the 6 µm voxel resolution of the inspection technique remains after the HIP.

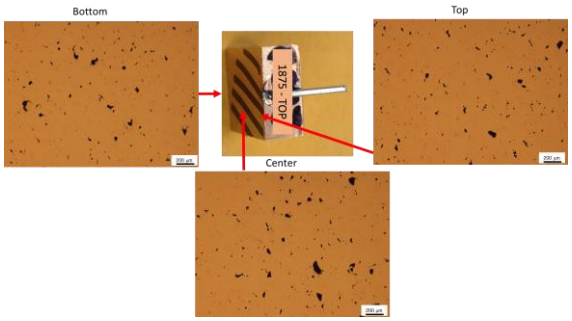

Fig 9: Extreme parameter set 1, as built sample pre-HIP.

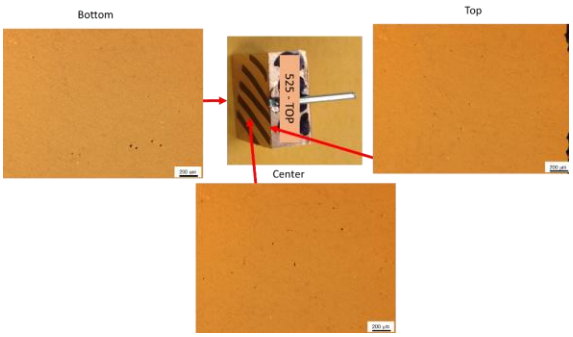

Fig. 10: Extreme parameter set 2, as built sample pre-HIP. Note - the dark spots on the right of the top image are the edge of the specimen, not pores.

Scanning Electron Microscopy (SEM) was performed on both pre and post-HIP specimens. This examination revealed the presence of Cr-rich precipitates that are not present pre-HIP, but are present post-HIP. Figures 11 and 12 are SEM images with Energy Dispersive X-ray Spectroscopy (EDS) spectra indicating chemistry of specific particles and the matrix in the image.

Figure 11 shows the pre-HIP microstructure. In this image the bright particles are Cr_2Nb as expected from previous work on GRCop-84 [6]. This was corroborated by examining Cr and Nb content identified by EDS. Additionally, the EDS analysis verified that the matrix surrounding the particles was primarily copper. Small amounts of Cr and Nb were detected due to the excitation volume likely including some subsurface Cr_2Nb particles.

Figure 12 shows a backscattered SEM image and associated EDS spectrum post-HIP. The key thing to note in this image is the presence of a dark phase that was not present prior to HIPing (see Figure 11). From the EDS spectrum, these dark precipitates are Cr-enriched precipitates. To verify the composition of these particles, several additional analysis techniques were employed. Data from electron microprobe, Auger spectroscopy, and x-ray diffraction all indicate that the dark phase, viewed in SEM backscattered mode, is elemental chromium. This is consistent with the deliberate biasing of the chemistry to a slightly Cr-rich composition to prevent hydrogen embrittlement[8,9]. Observations of the build also indicate that there may be Cu volatilization during LBM, which would effectively increase the Cr content.

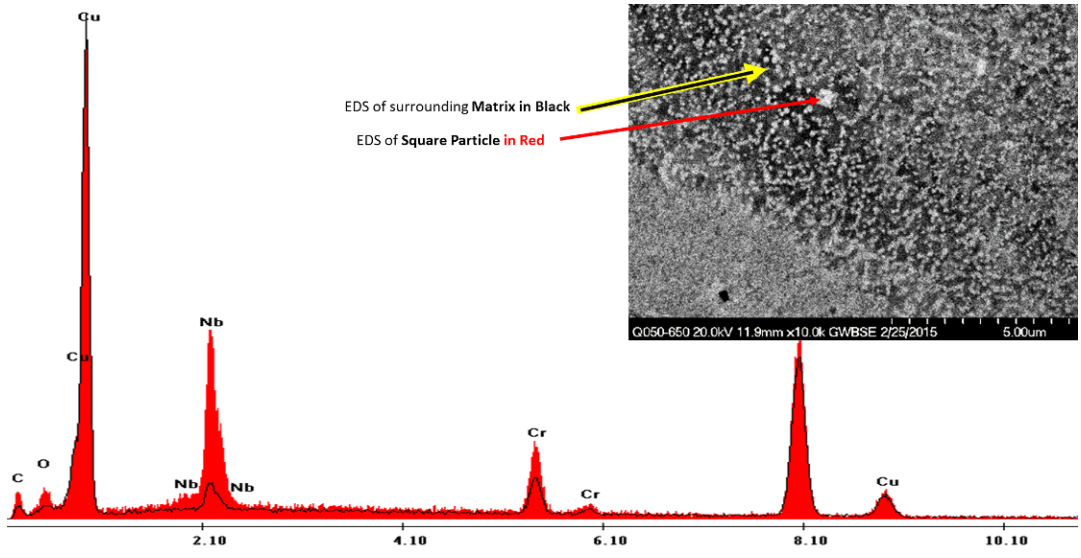

Fig. 11: Back-scatter Electron (BSE) image and EDS spectra of a pre-HIP specimen. The red spectrum shows the chemistry of a Cr2Nb particle, the black line indicates the chemistry of the surrounding copper matrix.

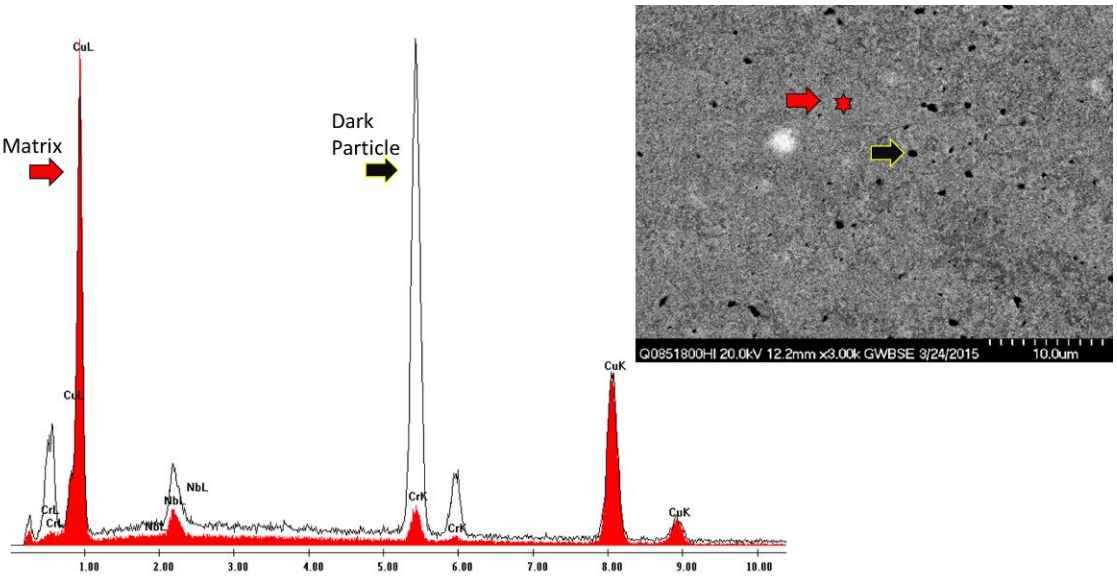

Fig. 12: Post-HIP Backscattered SEM image and EDS spectra showing the presence of chromium rich precipitates.

During LBM, the solid GRCop-84 part would act to quench the liquid metal and prevent precipitation of the Cr precipitates. During subsequent heating, the Cr would almost immediately precipitate based upon the Cu-Cr T-T-T curve[10]. This appears to be consistent with the observations.

Small amounts of Cr precipitates have been observed in the past but generally not reported due to their fine size and very low volume fraction[11]. There were no indications that they were deleterious to the mechanical properties of GRCop-84. Commercial Cu-Cr alloys such as Cu-0.9 Cr have excellent mechanical properties up to about 500 °C[12]. Morris and Morris also reported excellent properties for rapidly solidified Cu-Cr alloys[13]. Based upon past experience and the lack of a likely deleterious effect, the presence of elemental Cr precipitates is not viewed as a problem and may help to improve the properties of GRCop-84 as Cu_xZr precipitates do in the GRCop-84Z alloy[14].

Future work

As the project continues, characterization will be conducted on the LBM GRCop-84 combustion chamber liner. Specific work that is planned:

- HIPing process development continues on actual liners. A pathfinder liner has been produced by MSFC and will be used to improve HIPing process. In particular we will be evaluating dimensional changes and closure of porosity.
- Over 180 mechanical tests are planned. This includes tensile, fatigue, and compact tension specimens at relevant temperatures.

VI SUMMARY

NASA GRC is leveraging its technical expertise and capabilities in the areas of liquid rocket engine testing and detailed materials characterization to advance AM technology. An in-depth characterization of Electron Beam Melted (EBM) Ti-6Al-4V material has been completed. The mechanical properties of HIP'ed EBM Ti-6Al-4V were equivalent or superior to conventionally manufactured material. The high strength of the AM Ti-6Al-4V is attributed to the refined, lamellar microstructure. A significant difference in tensile strength was observed between the two lots of samples and was attributed to the crystallographic orientation with lot 1 having a strong fiber texture and lot 2 having a random texture. Inclusions, both low and high density, were present in the EBM Ti-6Al-4V but generally did not affect the mechanical properties of the alloy. The excellent mechanical properties of HIP'ed EBM Ti-6Al-4V are sufficient to design and manufacture quality aerospace components.

Work is ongoing to perform detailed microscopy, and perform mechanical properties testing for the GRCop-84 combustion chamber. To date microstructural results look promising and we have identified no significant technical hurdles that could impede production of the combustion chamber liner for NASA's STMD Low Cost Upper Stage Engine project.

In the four powder melts analyzed chemistry was within the specified range. Additionally, the impurity elements identified are not expected to result in deleterious metallurgical phases or a reduction in mechanical properties. Based upon past experience and the lack of a likely deleterious effect, the presence of elemental Cr precipitates in the post HIP microstructure is not viewed as a problem and may help to improve the properties of GRCop-84 as CuxZr precipitates do in the GRCop-84Z alloy.

VII REERENCES

1. Draper, S.L. et al: Proceedings of Ti-2015: The 13th World Conference on Titanium, TMS, 2015.
2. Draper, S.L. et al: NASA TM to be published in 2015.
3. Semiatin, S.L. and Bieler, T.R.: Metall. and Mat. Trans. A, 2001, vol. 32A, p.p. 1787-1799, 2001.
4. Nalla, R.K.; Boyce, B.L.; Campbell, J.O.; and Ritchie, R.O.: Metall. and Mat. Trans. A. 2002, vol. 33A, pp. 899-918.
5. Lutjering, F. and Albrecht, J; Titanium ’95: Science and Technology Proceedings from the Eighth World Conference on Titanium, ed. Blenkinsop, P.A. et al, 1995, pp. 1163-1170.
6. D.L. Ellis, “GRCop-84: A High Temperature Copper-based Alloy for High Heat Flux Applications,” NASA/TM-2005-213566, E-15011, Feb. 1, 2005.
7. D. Ellis et al, “A Practical Guide to the Production of Metal Spun NiCrAlY Coated GRCop-84 Liners,” NASA TM-2006-214123, April 2006. ITAR Restricted.
8. D.L. Ellis, A.K. Misra and R.L. Dreshfield, “Effect of hydrogen exposure on a Cu-8 Cr-4 Nb alloy,” NASA-TM-106429, E-8271, NAS 1.15:106429, Dec. 1, 1993.
9. D.L. Ellis and K. Hastings, “Effects of Hydrogen on GRCop-84,” NASA/TM-2006-214269, E-15555, Apr. 2006.
10. H. Suzuki and M. Kanno, “The T-T-T Curve In Cu-Cr Alloy”, Nippon Kinzuki Gakkaishi, Vol. 35, No. 5, (1981), pp 434-439. NASA Technical Translation NASA TT – 20167.
11. K.R. Anderson, J.R. Groza, R.L. Dreshfield, D. Ellis, “High-Performance dispersion-strengthened Cu-8 Cr-4 Nb alloy”, Met. and Matls. Trans. A, Sept. 1995, Vol. 26, Iss. 9, pp 2197-2206.
12. H.C. deGroh, D.L. Ellis and W.S. Loewenthal, “Comparison of GRCop-84 to Other High Thermal Conductive Cu Alloys,” NASA/TM-2007-214663, E-15798, Feb 1, 2007.
13. M.A. Morris, D.G. Morris, “Microstructures and mechanical properties of rapidly solidified Cu-Cr alloys”, Acta Metallurgica, Volume 35, Issue 10, October 1987, Pages 2511-2522, ISSN 0001-6160.
14. D.L. Ellis and BA. Lerch, “Improvement of GRCop-84 through the Addition of Zirconium”, NASA/TM-2012-216985, E-17626, June 1, 2012.